Iris Bulbs Express Type 1 and Type 2 Ribosome-Inactivating Proteins with Unusual Properties[1]

Qiang Hao, Els J.M. Van Damme*, Bettina Hause, Annick Barre, Ying Chen, Pierre Rougé, and Willy J. Peumans

Laboratory for Phytopathology and Plant Protection, Katholieke Universiteit Leuven, Willem de Croylaan 42, 3001 Leuven, Belgium (Q.H., E.J.M.V.D., Y.C., W.P.); Institute of Plant Biochemistry, P.O. Box 110432, D–06018 Halle, Germany (B.H.); and Institut de Pharmacologie et Biologie Structurale, Unité Propre de Recherche Centre National de la Recherche Scientifique 9062, 205 Route de Narbonne, 31077 Toulouse cedex, France (A.B., P.R.)

Two closely related lectins from bulbs of the Dutch iris (*Iris hollandica* var. Professor Blaauw) have been isolated and cloned. Both lectins, called Iris agglutinin b and Iris agglutinin r, possess *N*-glycosidase activity and share a high sequence similarity with previously described type 2 ribosome-inactivating proteins (RIP). However, these lectins show only 57% to 59% sequence identity to a previously characterized type 1 RIP from iris, called IRIP. The identification of the iris lectins as type 2 RIP provides unequivocal evidence for the simultaneous occurrence of type 1 and type 2 RIP in iris bulbs and allowed a detailed comparison of type 1 and type 2 RIP from a single plant, which provides further insight into the molecular evolution of RIP. Binding studies and docking experiments revealed that the lectins exhibit binding activity not only toward Gal/*N*-acetylgalactosamine, but also toward mannose, demonstrating for the first time that RIP-binding sites can accommodate mannose.

Many plants contain one or more so-called ribosome-inactivating proteins (RIP). RIP are *N*-glycosidases that catalytically inactivate eukaryotic ribosomes (Barbieri et al., 1993) by removing a single adenine residue from the large rRNA. RIP are divided into three groups on the basis of their molecular structure. Type 1 RIP are single chain proteins consisting of an enzymatically active polypeptide chain of approximately 30 kD. They are widespread among higher plants and occur in monocots as well as in dicots. Type 2 RIP are built up of one or more protomers consisting of two different disulfide-linked A and B chains. The A chain of the [A-s-s-B] pair shows sequence similarity to type 1 RIP and has RNA *N*-glycosidase activity, whereas the B chain is devoid of enzymatic activity, but contains carbohydrate-binding sites. Due to the presence of these carbohydrate-binding sites, type 2 RIP are also regarded as lectins (Peumans and Van Damme, 1995). Hitherto, type 2 RIP have been identified in *Abrus precatorius* (Fabaceae), *Adenia digitata* and *A. volkensii* (Passifloraceae), castor bean (Euphorbiaceae), *Viscum album* (Viscaceae), *Cinnamonum camphora* (Lauraceae), *Eranthis hyemalis* (Ranunculaceae), and *Sambucus nigra*, *Sambucus ebulus*, and *Sambucus sieboldiana* (Sambucaceae; Van Damme et al., 1998). The concept of type 3 RIP was introduced only recently after the discovery of RIP that are synthesized as single chain zymogens of about 30 kD and are converted into the enzymatically active form through a post-translational processing including the excision of a short internal peptide. Hitherto, type 3 RIP have been identified only in maize and barley (Mehta and Boston, 1998).

Though numerous RIP have been studied in detail, several important questions related to the biology of these proteins remain to be answered. A first question concerns the simultaneous occurrence of type 1 and type 2 RIP in plant tissues. It has been claimed that seeds of the camphor tree (Ling et al., 1995) and the leaves/bark of dwarf elder (Girbes et al., 1993; de Benito et al., 1995) and elderberry (de Benito et al., 1998) express simultaneously type 1 and type 2 RIP. However, the genes encoding the presumed type 1 RIP of *C. camphora* and *Sambucus* sp. have not been cloned yet and the amino acid sequence data are insufficient to trace their relationship with the type 2 RIP from the same species. A second question concerns the carbohydrate-binding specificity of the B chain of type 2 RIP. All type 2 RIP characterized hitherto contain binding sites that accommodate Gal or *N*-acetylgalactosamine (or both) except elderberry agglutinin I, which harbors a Neu5Ac(α, 2–6) Gal/GalNAc-binding site (Van Damme et al., 1996). Be-

[1] This work was supported in part by the Katholieke Universiteit Leuven (grant no. OT/98/17), by the Centre National de la Recherche Scientifique and Conseil Régional de Midi-Pyrénées (grants to A.B. and P.R.), by the Flemish Minister for Science and Technology (grant no. BIL98/10 to Y.C.), and by the Fund for Scientific Research-Flanders (grant no. G.0223.97). W.J.P. is Research Director and E.J.M.V.D. is a Postdoctoral Fellow of this fund. Q.H. acknowledges the receipt of a doctoral scholarship from the Research Council of the Katholieke Universiteit Leuven.

* Corresponding author; e-mail Els.VanDamme@agr.kuleuven.ac.be; fax 32–16–322976.

cause there are good indications from structural studies of other plant lectin families that even fairly well-conserved binding sites can exhibit a different specificity, it is questionable whether the specificity of type 2 RIP is really restricted to Gal, *N*-acetylgalactosamine, and Neu5Ac(α, 2–6) Gal/GalNAc. To answer these questions, novel plants containing RIP with unusual properties have to be studied.

This report deals with the cloning and characterization of two type 2 RIP from bulbs of iris (*Iris hollandica*). These iris type 2 RIP are unique because their binding sites accommodate Gal/GalNAc and also Man. Moreover, since iris bulbs contain a mixture of three typical type 1 RIPs (Van Damme et al., 1997a), the identification and cloning of the iris lectins provides for the first time unequivocal evidence for the simultaneous occurrence of type 1 and type 2 RIP in the very same tissue. In addition, detailed sequence and activity comparisons of the iris proteins yield novel insights in the occurrence and evolution of RIP.

RESULTS

Type 1 and Type 2 RIP Occur Simultaneously in Iris Bulbs

Iris bulbs express a natural mixture of three closely related isoforms of a typical type 1 RIP (called IRIP; Van Damme et al., 1997a). Because this type 1 RIP shares sequence similarity with one of the polypeptides of a previously isolated iris lectin (called IRA; Mo et al., 1994) the possible RIP activity of IRA was reinvestigated and the corresponding genes cloned.

Two isoforms of IRA were separated by elution from immobilized Gal with a gradient of increasing Gal concentration (Fig. 1A). SDS-PAGE revealed that the first eluting isoform consists of two different disulfide-linked polypeptides of 30 and 38 kD, respectively, whereas the second isoform is built up of two different disulfide-linked polypeptides of 30 and 35 kD, respectively (Fig. 1B). The first and second eluting isolectins apparently correspond to the column-retarded lectin (IRAr) and column-binding lectin (IRAb), respectively, obtained by Mo et al. (1994) by affinity chromatography on a column of protein A disaccharide (GalNAcα1, 3Gal). In accordance with this, the two isolectins of IRA will further be referred to as IRAr and IRAb. IRAr and IRAb eluted in a single symmetrical peak with an apparent M_r of approximately 65,000 upon gel filtration on a Superose 12 column (Fig. 1D), indicating that they consist of a single type 2 RIP protomer. Determination of the total carbohydrate content of IRAb and IRAr yielded values of 2.2% and 5.8%, respectively (corresponding to eight and 22 monosaccharides, respectively). Taking into account that plant *N*-glycans usually consist of seven to eight monosaccharides, IRAb and IRAr most probably contain one and three *N*-linked oligosaccharides, respectively. Since the deduced sequence of the A chain of IRAb and IRAr possess no putative *N*-glycosylation sites, all these glycans must be located on the respective B chains. The difference in degree of glycosylation explains the higher apparent molecular mass of the B chain of IRAr (38 kD) as compared with that of the B chain of IRAb (35 kD). N-terminal sequencing of the A and B chains of IRAb and IRAr yielded very similar though not identical sequences (Fig. 2), which showed little similarity with the corresponding parts of other type 2 RIP. However, sequencing of cyanogen bromide fragments of IRAb yielded two internal sequences with a fairly high similarity with parts of the A chain of ricin (Fig. 2).

Though reduced IRAb and IRAr behave like typical type 2 RIP upon SDS-PAGE, the unreduced iris lectins showed an aberrant polypeptide pattern. It is striking, indeed, that unreduced IRAb and IRAr yielded a prominent polypeptide of approximately 30 kD. Since this 30-kD polypeptide migrated at the same position as IRIP it was investigated whether the 30-kD band corresponded to contaminating IRIP (or another protein). Although contamination of IRAb and IRAr with IRIP is very unlikely because the lectins were isolated by a highly specific affinity chromatography procedure, additional experiments were carried out to rule out the possibility of such a contamination. First, the N-terminal sequence of the 30-kD polypeptide was determined. Because the obtained sequence matched that of the A chain of IRAb and IRAr, a major contamination of IRAb and IRAr with IRIP is very unlikely. Second, gel filtration of pure IRAb and IRAr and mixtures of IRAb/IRIP and IRAr/IRIP indicated that the pure lectins do not contain detectable quantities of IRIP (Fig. 1D). Third, western-blot analysis of IRAb and IRAr demonstrated that the 30-kD polypeptide of the reduced lectins does not cross-react with monospecific antibodies against IRIP (Fig. 1C). These observations clearly demonstrate that the 30-kD polypeptides visible in the SDS-PAGE pattern of unreduced IRAb and IRAr do not represent contaminating IRIP, but correspond to the A chain of the respective lectins.

The unusual behavior of the unreduced type 2 RIP upon SDS-PAGE is not fully understood. One possible explanation is the disruption of the inter-chain disulfide bridge between the respective A and B chains followed by the formation of an intra-chain disulfide bridge. The formation of such an intra-chain disulfide bond has not been observed yet for any type 2 RIP, but may take place in the A chain of IRAr and IRAb because they both contain two neighboring Cys residues at their respective C-termini (unlike all other type 2 RIPs, which contain only a single Cys residue at the C terminus of their A chain). The presumed formation of an intra-chain disulfide bridge within the A chains of IRAr and IRAb (Fig. 1B, lanes 3 and 4) also explains why they migrate slightly slower than their reduced counterparts (Fig. 1B, lanes

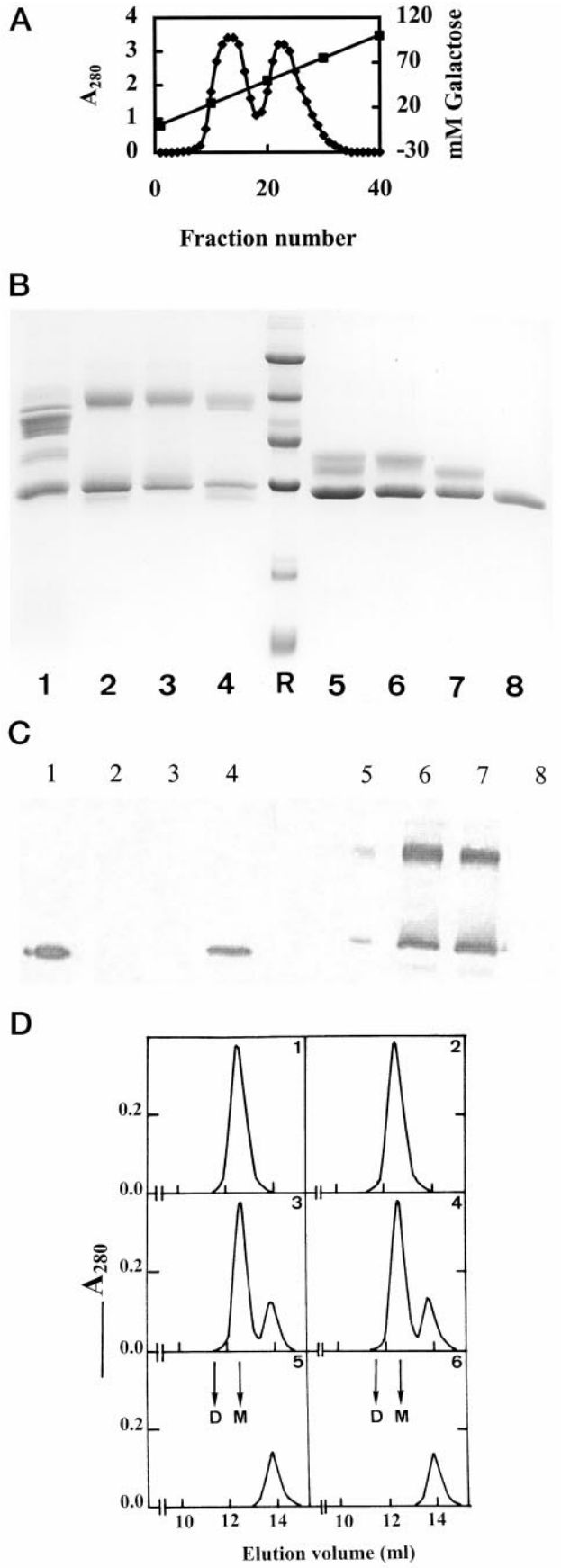

6 and 7). The free B chains released after disruption of the inter-chain disulfide bridge most probably associate covalently into dimers through the formation of a disulfide bridge between the free Cys residues at the N terminus of two B chains. PAGE under non-reducing conditions (i.e. in the absence of SDS) yielded a different result. Unreduced and reduced IRAr and IRAb migrated as a single polypeptide band (results not shown), indicating that no disruption takes place of the interchain disulfide bridge in the native (non-denatured) proteins, not even in the presence of 140 mM β-mercaptoethanol. It appears, therefore, that native IRAr and IRAb behave like other type 2 RIPs upon PAGE. However, after denaturation with SDS, the unreduced iris lectins show an aberrant polypeptide pattern upon SDS-PAGE.

Carbohydrate-Binding Properties of IRAb and IRAr

IRAb and IRAr agglutinated trypsin-treated rabbit erythrocytes equally well, with the minimal concentration required for activity being approximately 2.5 μg/mL. Hapten inhibition assays indicated that both lectins exhibit a very similar specificity toward Gal and *N*-acetylgalactosamine. The concentration required to inhibit the agglutination activity of trypsin-treated rabbit erythrocytes was 0.1 and 6 mM for *N*-acetylgalactosamine and Gal, respectively, for IRAb and IRAr (at a lectin concentration of 20 $\mu g\ mL^{-1}$).

Because docking experiments (see below) indicated that the binding sites of IRAr and IRAb can accommodate Gal/GalNAc as well as Man, the specificity of IRA for Man was checked. Hapten inhibition experiments yielded only a partial inhibition of the

Figure 1. A, Separation of IRAb and IRAr. Total affinity-purified IRA (in 1 M ammonium sulfate) was loaded on a column (2.6 × 20 cm; 100 mL bed volume) of Gal-Sepharose 4B and eluted with a linear gradient (400 mL) of increasing Gal concentration in 1 M ammonium sulfate. Fractions (10 mL each) were collected. B, SDS-PAGE of crude extracts and purified lectins from iris bulbs. Samples were loaded as follows: Lane 1, crude extract from iris bulbs; lanes 2 and 5, total IRA; lanes 3 and 6, IRAr; lanes 4 and 7, IRAb; and lane 8, IRIP. Samples in lanes 5 through 8 were reduced with β-mercaptoethanol. Molecular mass reference proteins (lane R) were lysozyme (14 kD), soybean trypsin inhibitor (20 kD), carbonic anhydrase (30 kD), ovalbumin (43 kD), bovine serum albumin (67 kD), and phosphorylase b (94 kD). C, Western-blot analysis of crude extracts and purified RIP of iris with antisera against IRIP (lanes 1–4) and IRA (lanes 5–8). Antisera were used in a dilution of 1:500. Samples were loaded as follows: lanes 1 and 5, crude extract of young developing iris bulbs; lanes 2 and 6, purified IRAr; lanes 3 and 7, purified IRAb; and lanes 4 and 8, purified IRIP. D, Gel filtration of purified IRAb and a mixture of purified IRAb and IRIP on a Superose 12 column. 1, 200 μg of purified IRAb; 2, 200 μg of purified IRAr; 3, 200 μg of purified IRAb mixed with 100 μg of purified IRIP; 4, 200 μg of purified IRAr mixed with 100 μg of purified IRIP; 5 and 6, 100 μg of purified IRIP. Arrows labeled D and M indicate the elution position of the dimeric and monomeric type 2 RIP SNAV (120 kD) and SNLRP (60 kD), respectively (both from elderberry; Van Damme et al., 1998).

```
LECIRAb: MHKKVNIKACLVSAIIWIWWAAIVGPAILVCSSSLSVTRGGHKNLPYKKV  50
LECIRAr:                    WAAIVGPAILVCSSSLLVTRDGHKYLNYDKV  31
RICIN:         MKPGGNTIVIWMYAVATWLCFGSTSGWSFTLEDNNIFPKQYPII  44
                             *           *.           *  .

LECIRAb: EFHITGCTKDTYSAFIQSLRTHLSSGT-SEYGIPLMRAQNPSSS-QELLL  98
LECIRAr: EFHITGCTKDTYSAFIQSLRTHLSSGT-SEYGIPLMRAQNPSSS-QQLLL  79
RICIN:   NFTTAGATVQSYTNFIRAVRGRLTTGADVRHEIPVLPNRVGLPINQRFIL  94
             .* *  .*. ** ..*  *..*.     **..        *  .*

LECIRAb: VEI------FGWDNEPVTLVLNLVNAYVIAYQAQGHYYLLHDTPDNPQLY 142
LECIRAr: VEI------FGWDNEPITLVVNLVNAYVIAYQAQNRYYLLHDTPDNPQLY 123
RICIN:   VELSNHAELSVTLALDVT------NAYVVGYRAGNSAYFFH--PDNQEDA 136
         **.           .*      ****. * *    *  *  ***

LECIRAb: GSDAHRLS--------FDGS-YPALQHVAGEYRENIDLGINELGSAILVL 183
LECIRAr: GSNPHRLS--------FDGS-YPALQRVAAENRENIELGINELGSAILVL 164
RICIN:   EAITHLFTDVQNRYTFAFGGNYDRLEQLAGNLRENIELGNGPLEEAISAL 186
             *  .          *  *  *  .*   ****.**   *  **  *

LECIRAb: HQWSPP-TVERTVARSFIVLIQMVSEAARFRAIETRVRRNIIQVGDYRSF 232
LECIRAr: HQWSPP-TVERSVARSLIVLIQMVSEVARFRAIETRVRRNIIQVGDYRSF 213
RICIN:   YYYSTGGTQLPTLARSFIICIQMISEAARFQYIEGEMRTRIRYN---RRS 233
            *   *   ..*** *. ***.** ***  **   *  *      *

LECIRAb: RPGAGMLDLETNWGTLSERVQESNEGVFANRLTLQTTNFETIHIYNAQTA 282
LECIRAr: RPGAGMLDLETNWEPLSERVQESNEGVFANRLTLQTSNFETIDIYNAQTA 263
RICIN:   APDPSVITLENSWGRLSTAIQESNQGAFASPIQLQRRNGSKFSVYDV--S 281
          *   .. **  *  **  .**** * **  . **  *     .*

LECIRAb: RQVCGLALLLFACKARQSLQALLPPHDSPVLPTLLDLNVVRSMLDIVEDD 332
LECIRAr: RQVCGLALLLFACKARQSLQALLPPHDSPVLPTLLDLNVVRSMLDIVEDD 313
RICIN:   ILIPIIALMVYRCAPPPSSQFSLLIR--PVVPNFN-------------AD 316
           .  .**..  *    * *  *     **.*                 *

LECIRAb: TCPVSEPTMRISGRDGYCMDVKDGLYHNGNPVTLSSCKQNNDVNQFWTFK 382
LECIRAr: TCPLSEPTMRISGRDGYCMDVKDGLYHNGNPVTLSSCKQNNDVNQFWTFK 363
RICIN:   VCMDPEPIVRIVGRNGLCVDVRDGRFHNGNAIQLWPCKSNTDANQLWTLK 366
          *   ** .** ** * *.**.**  **** . *  ** * * ** ** *

LECIRAb: SDGTIQSNGKCLTAYGYNAGAYVMIYDCSSAVMGATLWTMY-NGSLINRP 431
LECIRAr: SDGTIQSNGKCLTAYGYNAGAYVMIYDCSSAVMGATLWTMY-NGSLINRP 412
RICIN:   RDNTIRSNGKCLTTYGYSPGVYVMIYDCNTAATDATRWQIWDNGTIINPR 416
          * ** *******.***  * ******* .*   ** * .  **..**


LECIRAb: SGLAISAESGESGTTLTMQVHLNASKQGWLPSNNTRPFLTPIIGINGLCV 481
LECIRAr: SGLAISAESGESGTTLTMQVHLHASKQGWLPSNNTRPFLTPIIGLNGLCM 462
RICIN:   SSLVLAATSGNSGTTLTVQTNIYAVSQGWLPTNNTQPFVTTIVGLYGLCL 466
         * * ..* ** ******.*  . *  *****.*** **.* *.*. ***.

LECIRAb: QRNDQEDVGLATCDDNNSNQKWYLYGDGSIRPLTDPNYCVTSQTHDQGSQ 531
LECIRAr: QRNDQEDVGLVTCDDNNSNQKWYLYGDGSIRPLIDPTYCVTSQTHDQGSQ 512
RICIN:   QANS-GQVWIEDCSSEKAEQQWALYADGSIRPQQNRDNCLTSDSNIRETV 515
         * *    * .  *       * * ** ******       *.** .    .

LECIRAb: IILLSCNFGGASQRWMFTSQGTIYNLHSGYVMDVKQSDPSLQQIIIWSTT 581
LECIRAr: IILLSCNFGGASQRWMFTSQGTIHNLHSGYVMDVKQSDPSLQQIIIWSTT 562
RICIN:   VKILSCGPASSGQRWMFKNDGTILNLYSGLVLDVRASDPSLKQIILYPLH 565
         . .***    . *****   *** ** ** *.**. ***** ***.

LECIRAb: GNPNQMWFTTF 592
LECIRAr: GNPNQMWFTTF 573
RICIN:   GDPNQIWLPLF 576
         * ***.*.  *
```

Figure 2. Comparison of the deduced amino acid sequences of the cDNA clones encoding IRA and ricin. The arrowhead indicates the processing site for the cleavage of the signal peptide. Dashes denote gaps introduced to obtain maximal homology. Putative *N*-glycosylation sites in the iris sequences are indicated in bold. The N-terminal amino acid sequences of the A and B chains of the iris type 2 RIP are underlined. Sequences of CNBr fragments of IRAb are also underlined in the deduced sequence of *LECIRAb*. Asterisks under the IRA and ricin sequences denote identical amino acid residues, whereas highly homologous amino acids are indicated by dots.

agglutination of rabbit and human erythrocytes at high concentrations (>0.1 M) of Man, indicating that free Man cannot out compete the glycan receptors on the surface of the red blood cells. To check the presumed Man-binding activity of the iris lectins, affinity chromatography experiments were done using immobilized Gal and Man. Total IRA was quantitatively retained on Sepharose 4B-Gal and Sepharose 4B-Man (at least in the presence of 1.2 M ammonium sulfate). Moreover, the bound lectins were desorbed when the columns were eluted with a 0.1 M solution of the free sugar in 1.2 M ammonium sulfate (results not shown).

Enzymatic Activity and Cytotoxicity of IRAb and IRAr

The RNA *N*-glycosidase activity of IRIP and a total preparation of IRA (mixture of IRAb and IRAr) was checked using animal and plant ribosomes as substrates. Both RIP were highly active on rabbit reticulocyte and wheat germ ribosomes. A 400-bp RNA fragment in case of rabbit reticulocyte ribosomes and a 350-bp fragment for wheat germ ribosomes (i.e. the so-called Endo-fragments) clearly appeared in the electropherogram of the rRNA after treatment with acidic aniline (Fig. 3). It should be noted that the native (i.e. unreduced) and the reduced form of IRA exhibit enzymatic activity. The minimal concentration of IRIP and IRA required for activity toward plant ribosomes is about 100,000-fold higher than that for animal ribosomes, being 200 nM and 2 pM for IRIP and 2,000 nM and 20 pM for IRA, respectively. IRA is apparently less active than IRIP on animal and plant ribosomes. To check whether IRAb and IRAr have *N*-glycosidase activity, the same experiments were repeated with the purified isoforms. Both lectins deadenylated wheat germ and rabbit ribosomes, with the minimal concentrations required for activity

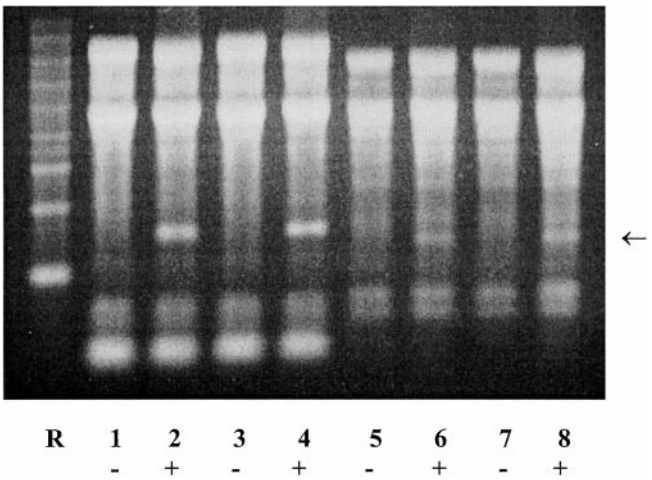

Figure 3. RNA *N*-glycosidase activity of IRA (mixture of IRAr and IRAb) and IRIP toward animal (lanes 1–4) and plant (lanes 5–8) ribosomes. Ribosomes were incubated with 2 μM IRIP (lanes 1 and 2 and 5 and 6) or 2 μM IRA (lanes 3 and 4 and 7 and 8). Following incubation, rRNA was extracted, treated with acidic aniline, and was separated on an agarose-formamide gel. RNA bands were visualized by ethidium bromide staining. (+) and (−) indicate aniline treatment or absence of aniline treatment. The arrow indicates the position of the Endo's band released from the ribosomes by aniline treatment of the modified rRNA. Lane R shows an RNA marker with fragments of 281, 623, 955, 1,383, 1,908, 2,604, 3,638, 4,981, and 6,583 nucleotides (Promega, Madison, WI).

being 2,000 nM and 20 pM, respectively (results not shown), indicating that IRAb and IRAr are equally active.

Cytotoxicity tests revealed that IRAb and IRAr exhibit a low toxicity toward cell lines L1210/0, FM3A/0, Molt4/C8, and CEM/0 (Table I). The slightly higher (2–5 times) cytotoxicity of the lectins is in good agreement with the general observation that type 2 RIP are more toxic than type 1 RIP. It should be emphasized, however, that IRAr and IRAb are at least three orders of magnitude less toxic than the toxic mistletoe type 2 RIP ML-II.

Cloning of the Genes Encoding IRAb and IRAr

A cDNA library was screened using an oligonucleotide derived from the sequence of a CNBr fragment of the B chain of the iris type 2 RIP. Sequence analysis revealed the occurrence of two groups of cDNA clones (called *LECIRAb* and *LECIRAr*, respectively) encoding proteins containing the N-terminal sequences of IRAb and IRAr, respectively (Fig. 2). *LECIRAb* contains a 1,779-bp open reading frame encoding a polypeptide of 593 amino acids with one possible initiation codon at position 2 of the deduced amino acid sequence. Assuming that this Met is used as the translation initiation site, the primary translation product is a polypeptide of 592 amino acids (65,676 D). The sequence from amino acid 45 to 74 matches exactly the amino acid sequence of the A chain of IRAb. A closer analysis of the sequence reveals a stretch of amino acids (residues 329–338) corresponding to the N-terminal sequence of the B chain of IRAb. The B chain has a calculated molecular mass of 29,066 D (264 amino acids), whereas the calculated molecular mass of the A chain with the linker sequence is 31,886 D.

The second group of cDNA clones (*LECIRAr*) encodes a precursor polypeptide of 573 amino acids with a calculated molecular mass of 63,758 D. A closer analysis of the deduced sequence revealed that *LECIRAr* contains two stretches of amino acids (residues 28–53 and residues 310–319, respectively) corresponding to the N-termini of the A and B chain of IRAr, respectively. Judging from the sequence similarity with *LECIRAb*, *LECIRAr* lacks the start codon and the first amino acid residues of the signal peptide. The calculated molecular mass for the A chain (containing the linker sequence) and the B chain is 31,773 and 29,136 D (264 amino acids), respectively. Sequence comparison of IRAb and IRAr revealed 96.0% sequence similarity (94.6% sequence identity). Clones *LECIRAb* and *LECIRAr* cross-hybridize, but show no cross reactivity with clones encoding IRIP from iris.

Northern-Blot Analysis

Hybridization of a northern blot using the random primer-labeled cDNA encoding the RIP genes of iris as a probe yielded a signal of approximately 2 kb (results not shown). This result was identical when hybridization was performed using the oligonucleotide used for screening of the cDNA library. On the blot there was no cross-hybridization with the mRNAs encoding IRIP.

Western Blot

Because IRIP and the A chain of IRAr and IRAb share a reasonably high sequence similarity (57.4% sequence identity and 67.5% sequence similarity for IRAb; 59.2% sequence identity and 68.2% sequence similarity for IRAr) the possible serological relationship between both proteins was investigated by double immunodiffusion (results not shown) and western-blot (Fig. 1C) analysis. No cross-reaction was observed with either technique, indicating that IRA and IRIP share no common epitopes with the particular antisera that were used.

Molecular Modeling of the IRAb and IRAr

Hydrophobic cluster analysis (HCA) plots of the A and B chains of both isoforms of IRA look very similar to those of ricin (results not shown). In accordance with this, accurate three-dimensional models of both isoforms of IRA could be built by homology modeling from the x-ray coordinates of ricin. In this section the numbering of amino acids refers to the position of the amino acid along the mature A and B chain of the RIP.

In spite a few insertions and deletions, which are mainly located in loop regions, the A chains of IRAr and IRAb exhibit a three-dimensional fold very similar to that of the A chain of ricin (Fig. 4A). All the amino acid residues forming the active site of the ricin A chain are conserved in the A chain of IRAr (Tyr-73, Tyr-109, Glu-162, Arg-165, and Trp-199) and IRAb (Tyr-75, Tyr-111, Glu-164, Arg-167, and Trp-

Table I. *Cytotoxic effect of IRIP, IRAb, and IRAr on human and animal cells*

Compound	IC50 ($\mu g\ mL^{-1}$)			
	L1210/0	FM3A/0	Molt4/C8	CEM/0
IRAb	37 ± 12	17 ± 10	6.5 ± 0.05	7.0 ± 0.04
IRAr	48 ± 20	33 ± 20	4.9 ± 0.3	6.7 ± 0.3
IRIP	76 ± 25	69 ± 44	25 ± 1	19 ± 4
ML-II	0.015 ± 0.0004	0.62 ± 0.02	<0.005	<0.005

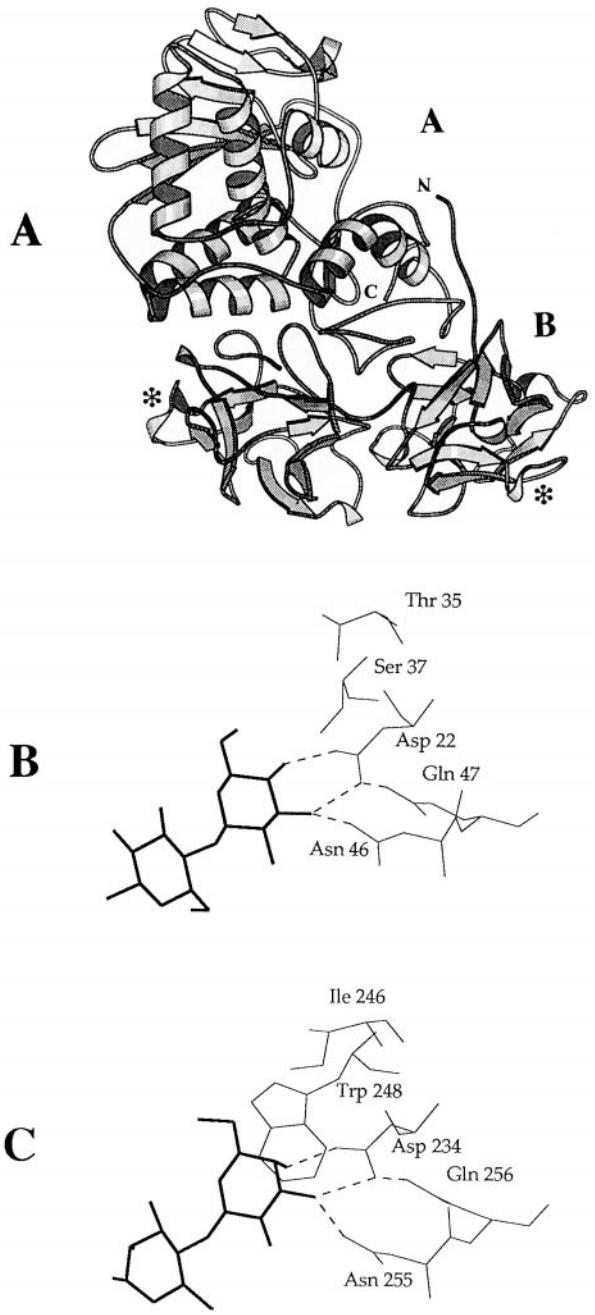

Figure 4. Three-dimensional model showing the A (A) and B (B) chain of IRAr. The six strands of β-sheet of the A chain exhibiting a left-handed twist and strands of β-sheet of the B chain are indicated by arrows and the two carbohydrate-binding sites are indicated by asterisks. Both chains are linked by a disulfide bridge between Cys-249 at the C terminus of the A chain and Cys-6 at the N terminus of the B chain. Cartoons were rendered with Molscript (Kraulis, 1991). Docking of lactose (thick lines) into the carbohydrate-binding sites numbered 1 (B) and 2 (C) of the B chain of IRAr was performed assuming that the orientation of lactose in the sites of ricin is conserved in IRA. The hydrogen bonds connecting the Gal moiety of lactose to the amino acid residues (tin lines) forming the binding sites of IRAr are indicated by dotted lines.

201). Most of the additional residues participating in the active site are also conserved in IRAr (Asn-71, Arg-120, Gln-158, Val-163, Glu-196, and Thr-197) and IRAb (Asn-73, Arg-122, Gln-160, Ala-165, Glu-198, and Thr-199). One can reasonably expect, therefore, that IRAr and IRAb possess *N*-glycosidase activity, which is in good agreement with the results of the *N*-glycosidase activity test.

The B chains of IRAr and IRAb consist like the B chain of ricin of two domains containing short strands of β-sheet interconnected by turns and loops (Fig. 4B). Each domain consists of three subdomains homologous to the corresponding subdomains of the ricin B chain. The B chain of IRAb and IRAr contains a Cys residue at position 6 that is at a Cα-Cα distance of 4.50 Å from the facing Cys located at positions 251 and 249 of the A chain of IRAb and IRAr, respectively. As a result, disulfide bonds can be formed between Cys-249-Cys-6 and Cys-251-Cys-6 of the A and B chains of IRAr and IRAb, respectively.

A few amino acid residues of the two presumed carbohydrate-binding sites, which are located at the N- and C-terminal subdomains of the B chains of IRAr and IRAb differ from those found in the corresponding sites of ricin. The most pronounced changes occur in the low affinity site of domain 1, in which Thr-37 and Ser-39 of IRAb and IRAr replace the corresponding Gln-35 and Trp-37, respectively, of ricin. Docking experiments showed that these changes prevent the formation of the hydrogen bond that connects O6 of Gal to Gln-35 of ricin with Thr-37 of the B chains of IRAr or IRAb. In addition, the stacking between the pyranose ring of Gal and Trp-37 of ricin is also not possible with Ser-39 of the B chains of IRAb or IRAr (Fig. 4B). In accordance with this, site 1 of the B chain of IRAb and IRAr is most likely only weakly active or even inactive. In site 2 of the B chain of IRAb and IRAr only a single amino acid residue is changed as compared with ricin (Tyr-248 of ricin is substituted by a Trp-250 residue; Fig. 4C). Docking experiments indicated that the network of hydrogen bonds connecting Gal to the amino acid residues of the site is not affected because Trp-250 stacks similarly to the pyranose ring of the sugar as Tyr-248 of ricin. More importantly, the replacement of Ala-237 of ricin by Gln-239 in the B chain of IRAr and IRAb causes a steric clash (1.72 Å) with O2 of the Glc moiety of lactose. As pointed out by Lehar et al. (1994), Ala-237 forms together with Arg-236 and Ser-238 a kink at the bottom of the sugar-binding pocket of site 2 of ricin. The replacement in ricin by site-directed mutagenesis of Ala-237 by a negatively charged and more bulky Asp residue creates a steric clash that strongly reduces the sugar-binding activity of site 2 of ricin. For this reason, site 2 of the B chain of IRAr and IRAb is suspected to be only moderately active. It is surprising that docking experiments performed with Man suggested that both carbohydrate-binding sites of IRA can accom-

modate Man. The network of hydrogen bonds connecting Man to sites 1 and 2 of IRA is similar to that observed for Gal. However, due to the axial position of O2 in Man, two additional hydrogen bonds can be formed between O2 of Man and the NH of Gly-26 and N2 of Asp-46 of site 1, and NH of Ser-238 and N2 of Asn-255 of site 2, respectively. Although the equatorial position of O4 of Man (axial position in Gal) introduces no change in the hydrogen bond connecting O4 to both sites, the shortest bond length is observed for Gal.

Phylogeny of IRIP and IRA

To trace the evolutionary relationships between IRA, IRIP, and other type 1 and type 2 RIPs, phylogenetic trees were built from the amino acid sequences of the A and B chains of type 2 RIP and type 1 RIP from different plant families. As shown in Figure 5, the A chain of IRA clusters together with IRIP in a single side branch of the main tree, suggesting that IRIP is more closely related to the A chain of IRA than to any other type 1 RIP. The B chain of IRA clusters in the same side branch as the B chains of ricin (Euphorbiaceae) and abrin (Leguminosae). This is rather surprising because one would expect that IRA is more closely related to the only known monocot type 2 RIP from *Polygonatum multiflorum* (Liliaceae; Van Damme et al., 2000) than to type 2 RIP from dicots.

DISCUSSION

Molecular cloning and activity analysis unambiguously demonstrated that iris bulbs express two closely related though different type 2 RIPs possessing RNA *N*-glycosidase as well as lectin activity. IRAr and IRAb closely resemble other type 2 RIPs with respect to their structure and specificity. It is surprising, however, that both binding sites of the B chain of IRAr and IRAb can, according to docking experiments, readily accommodate Man. Since this presumed Man-binding activity was confirmed by binding experiments on immobilized Man, the iris lectins illustrate for the first time that the specificity of the carbohydrate-binding motif of type 2 RIP is not necessarily confined to Gal/GalNAc, but may extend to other sugars. Type 2 RIP from elderberry, Solomon's seal, mistletoe, and castor bean did not show any binding activity toward Man under the same conditions, indicating that the Man-binding activity of the iris lectins is unique, indeed, among type 2 RIP.

Molecular cloning of IRA allowed for the first time the corroboration of structural and evolutionary relationships between type 1 and type 2 RIP from the same species. The sequence identity between IRIP and the A chain of IRAr and IRAb is only 57% to 59%. Compared with the sequence identity of the three isoforms of IRIP (90%) and the two isoforms of IRA (95%), the sequence similarity between iris type 1 and type 2 RIP is relatively low. This obvious lack of identity also explains why IRA does not cross react with monospecific antibodies against IRIP and vice versa.

The discovery and cloning of type 1 and type 2 RIP from a single plant allows re-addressing the question of the molecular evolution of RIP. IRIP is most closely related to the A chain of IRA, and surprisingly exhibits a relatively low sequence similarity with type 1 RIP from monocot species. It is also noteworthy that the B chain of IRA has the highest similarity with the B chains of type 2 RIP from the dicots castor bean and *A. precatorius*, and not with the B chain of the only known monocot type 2 RIP from *P. multiflorum* (Van Damme et al., 2000). These observations suggest that IRIP and IRA did not evolve separately from an ancestral type 1 and type 2 RIP (common to monocots and dicots), but arose from each other as a result of relatively recent evolutionary event. Because iris contains a type 1 and a type 2 RIP, but no lectin(s) consisting of subunits corresponding to the B chain of IRA, it is not self-evident that IRA arose from a gene fusion between IRIP and a hypothetical lectin. It seems more logic, indeed, that the IRIP gene originated from an (ancestral) IRA gene through the deletion of the B chain. Evidence for the evolution of RIP/lectin genes through a domain-deletion event has been obtained previously from the observation that one of the elderberry lectins is encoded by a truncated type 2 RIP gene in which almost the complete A domain is deleted (Van Damme et al., 1997b).

It should be emphasized that the proposed origin of IRIP from IRA through the deletion of the B chain applies exclusively to the evolution of the iris RIP. Taking into consideration the high degree of sequence conservation within the family of type 2 RIP, there is little doubt that there has been a common ancestor for all modern type 2 RIPs. Most probably, this common ancestor arose through a gene fusion between an ancestral type 1 RIP and an unrelated ancestral carbohydrate-binding protein. However, in some particular cases (e.g. in iris), a type 2 RIP gene gave raise through the deletion of the B-domain to a truncated gene encoding a type 1 RIP homolog. To further corroborate the proposed conversion of type 2 into type 1 RIP genes by domain-deletion events, additional species in which both types of RIP occur simultaneously should be studied. Besides iris, unfortunately, no such systems have been documented. There have been reports on the isolation and characterization of type 1 RIP from elderberry that coexist with type 2 RIP and related lectins (de Benito et al., 1995, 1998). However, the presumed identity of these elderberry type 1 RIPs awaits confirmation by sequence data. The same holds true for a type 1 RIP that occurs in combination with a type 2 RIP in seeds of *C. camphora* (Ling et al., 1995).

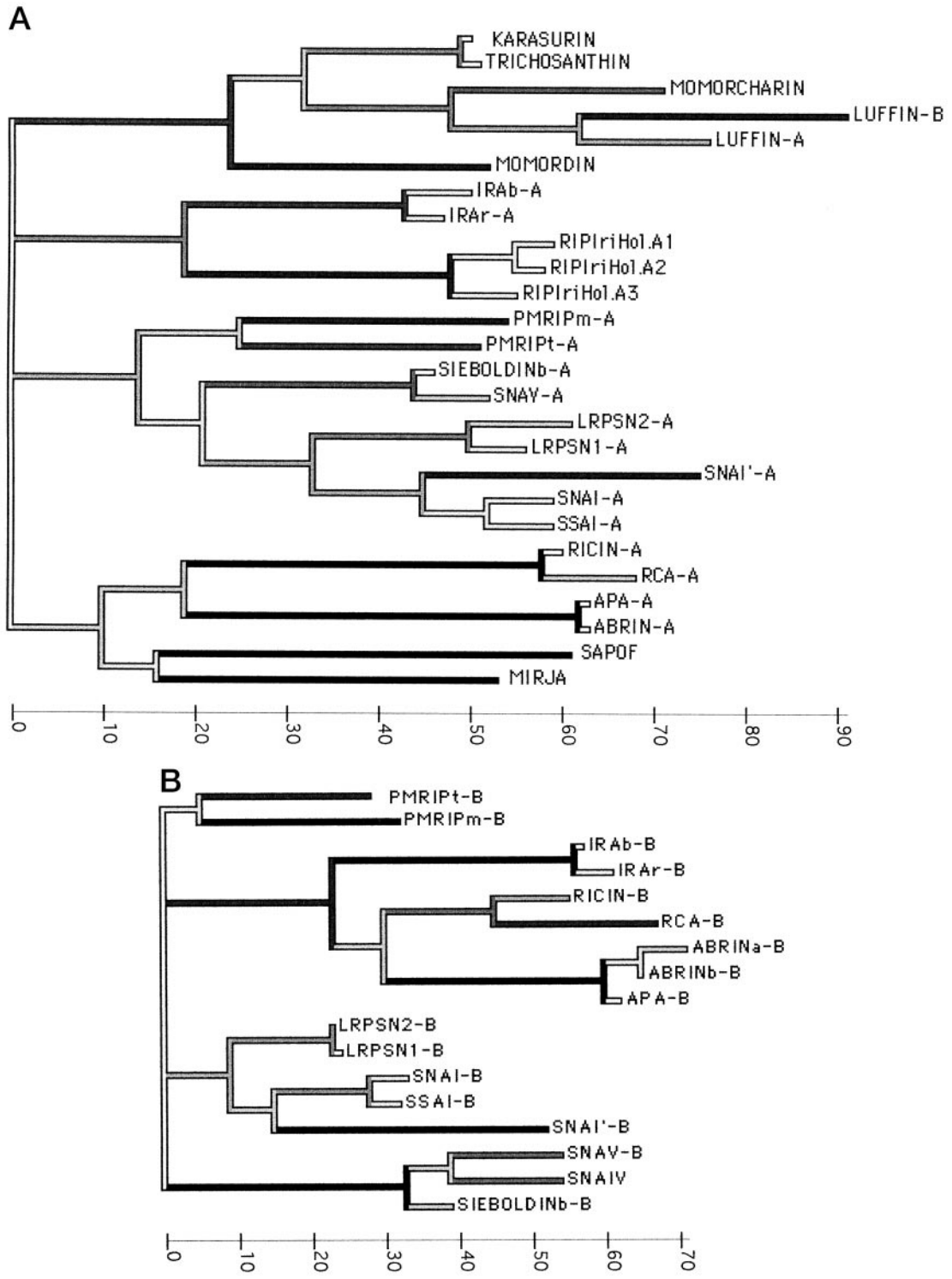

Figure 5. Phylogenetic trees built from the amino acid sequences of type 1 RIP or A chains (A) and B chains (B) of type 2 RIP (ricin-A, ricin-B, and lectin RCA-A and RCA-B from castor bean; abrin-A, abrina/b-B, and agglutinin APA-A and APA-B from *A. precatorius*; SNAI-A and SNAI-B, SNAV-A and SNAV-B, SNAI'-A and SNAI'-B, LRPSN1-A and LRPSN1-B, LRPSN2-A and LRPSN2-B, and SNA-IV from *S. nigra*; sieboldinb-A, sieboldinb-B, SSAI-A, and SSAI-B from *S. sieboldiana*; momordin and momorcharin from *Momordica charantia*; MIRJA from *Mirabilis jalapa*; PMRIPm-A and PMRIPm-B, PMRIPt-A and PMRIPt-B from *Polygonatum multiflorum*; RIPIriHol.A1, RIPIriHol.A2, and RIPIriHol.A3 from iris hybrid; IRAr-A and IRAr-B, IRAb-A and IRAb-B from iris hybrid; SAPOF from *S. officinalis*; luffin-A and luffin-B from *Luffa cylindrica*; and karasurin and trichosanthin from *Trichosanthes kirilowii*). Branches of the trees are shaded according to the amount of amino acid changes and the scales indicate the number of amino acid changes.

MATERIALS AND METHODS

Plant Material

Iris (*Iris hollandica* var. Professor Blaauw) bulbs were purchased from a local garden center in Belgium and kept at 2°C for 4 weeks. After vernalization the bulbs were transferred to pot soil and grown in a greenhouse. Approximately 4 weeks after flowering, developing bulbs were collected, peeled, and used immediately or stored at −80°C. Bulbs destined for the isolation of RNA were cut in small pieces and frozen in liquid nitrogen.

Isolation of Iris Agglutinin and IRIP from Bulbs

IRIP was isolated as described previously (Van Damme et al., 1997a). IRA was purified by affinity chromatography on Gal-Sepharose. Frozen developing iris bulbs (200 g) were homogenized with a Waring blender in 1 L of 20 mM Tris-HCl, pH 7.5, containing 0.2 M NaCl and the homogenate was centrifuged (9,000*g* for 10 min). The supernatant was brought at 1 M ammonium sulfate, cleared by centrifugation (9,000*g* for 15 min), and applied onto a column (2.6 × 10 cm; 50 mL bed volume) of Gal-Sepharose 4B equilibrated with 1 M ammonium sulfate. After washing the column with 1 M ammonium sulfate until the A_{280} fell below 0.01, the bound IRA was desorbed with a solution of 0.1 M Gal in 1 M ammonium sulfate. The affinity-purified lectin was loaded onto a column (1.6 × 10 cm; 20 mL bed volume) of Phenyl-Sepharose (Amersham Pharmacia Biotech, Uppsala) equilibrated with 1 M ammonium sulfate. After washing the column with 1 M ammonium sulfate the lectin was desorbed with 20 mM Tris-HCl, pH 8.7, dialyzed against appropriate buffers, and was stored at −20°C until use.

Separation of Total IRA into Two Isoforms

Three hundred milligrams of total affinity-purified IRA dissolved in 50 mL of 20 mM Tris-HCl (pH 8.7) was mixed with an equal volume of 2 M ammonium sulfate and loaded on a column (2.6 × 20 cm; 100 mL bed volume) of Gal-Sepharose 4B equilibrated with 1 M ammonium sulfate. After loading the lectin, the column was eluted with a linear gradient (400 mL) of increasing Gal concentration in 1 M ammonium sulfate. Fractions (10 mL each) were collected and the eluting proteins were analyzed by SDS-PAGE. As shown in Figure 1, IRAr and IRAb were reasonably well resolved.

Binding of IRA onto Immobilized Gal and Man

Total affinity-purified IRA (50 mg) dissolved in 20 mL of 1.2 M ammonium sulfate was loaded on a column (2 cm × 3 cm; approximately 10 mL bed volume) of Sepharose 4B-Gal or Sepharose 4B-Man. The bound lectin was desorbed with 0.1 M Gal or 0.1 M Man in 1.2 M ammonium sulfate. Fractions were collected and the A_{280} was measured.

Analytical Methods

Purified proteins were analyzed by SDS-PAGE with 15% (w/v) acrylamide gels using a discontinuous system. PAGE under non-denaturing conditions was done using 8% (w/v) acrylamide gels in Tris-HCl, pH 8.7. For N-terminal sequencing samples of IRAb and IRAr were separated by SDS-PAGE and electroblotted on a polyvinylidene difluoride membrane. Polypeptides were excised from the blots and sequenced on an protein sequencer (model 477A, Applied Biosystems, Foster City, CA) interfaced with an on-line analyzer (model 120A, Applied Biosystems). To obtain additional sequence information, IRAb and IRAr were cleaved with CNBr-cleavage and the fragments were sequenced. Therefore, lyophilized lectin (2 mg) was dissolved in 0.1 mL of 70% (w/v) formic acid. Ten milligrams of solid cyanogen bromide was added and the mixture was incubated overnight at 37°C (in the dark). Peptides were recovered by evaporation under vacuum, separated by SDS-PAGE, electroblotted, and were sequenced as described above.

Total neutral sugar was determined by the phenol/H_2SO_4 method with D-Glc as standard (Dubois et al., 1956).

Preparation of Monospecific Antibodies

Primary antibodies against IRIP and (total) IRA were raised in male New Zealand white rabbits. Rabbits were injected subcutaneously with 1 mg of purified protein dissolved in phosphate-buffered saline and emulsified in 1 mL of Freund's complete adjuvant. Four booster injections (with 1 mg of purified protein dissolved in phosphate-buffered saline) were given with 10-d intervals. Ten days after the final injection, blood was collected from an ear marginal vein. Serum was collected by centrifugation and the antibodies were purified by affinity chromatography on the immobilized antigen. The monospecificity of the antiserum was checked by western-blot analysis (Fig. 1C).

RNA *N*-Glycosidase Activity Assay and Cytotoxicity Test

Rabbit reticulocyte ribosomes and wheat germ ribosomes were prepared as described previously (Walthall et al., 1979; Sambrook et al., 1989) and stored in small aliquots at −80°C until use. The RNA *N*-glycosidase activity of the RIP was determined by the method of Endo and Tsurugi (1987) with minor modifications (Van Damme et al., 2000). IRIP, IRAr, and IRAb were evaluated for cytotoxic/cytostatic activity against murine leukemia L1210, murine mammary carcinoma FM3A, and human T-lymphocyte Molt 4/clone 8 and CEM cells as previously described (Van Damme et al., 2000).

RNA Isolation

Young developing bulbs were powdered in liquid nitrogen and total RNA was extracted (Van Damme et al., 1997a). Poly(A)-rich RNA was isolated by affinity chroma-

tography on oligo(deoxythymidine)-cellulose (Sigma, St. Louis).

Construction and Screening of cDNA Library

A cDNA library was constructed with poly(A)-rich mRNA from young developing bulbs using a cDNA synthesis kit (Amersham Pharmacia Biotech, Uppsala). cDNA fragments were inserted into the *Eco*RI site of PUC18. The library was propagated in *Escherichia coli* XL1 Blue (Stratagene, La Jolla, CA). The cDNA library was initially screened with a ^{32}P-labeled synthetic oligonucleotide derived from the sequence of a CNBr fragment of the B chain of the iris type 2 RIP (YHNGNPV, 5′ CAN GGG/A TTN CCG/A TTG/A TGG/A TA 3′). All colonies that reacted positively were selected and rescreened at low density using the same conditions. Plasmids were isolated from purified single colonies on a miniprep scale using the alkaline lysis method as described by Mierendorf and Pfeffer (1987).

Sequencing of cDNA Clones

Manual sequencing of both ends of the cDNA clones was performed by the dideoxy method (Sanger et al., 1977). The complete sequence of the cDNA clones encoding IRA was determined on an ABI 373A sequencer (Applied Biosystems, Eurogentec, Seraing, Belgium) and the open reading frame was translated. The deduced amino acid sequences were analyzed using programs from PC GENE (Biomed, Geneva) and GENEPRO (Riverside Scientific, Seattle).

Northern Blot

RNA electrophoresis was performed according to Sambrook et al. (1989). Approximately 3 μg of poly(A)-rich RNA was denatured in glyoxal and dimethylsulfoxide and separated in a 1.2% (w/v) agarose gel. Following electrophoresis the RNA was transferred to Immobilon N membranes (Millipore, Bedford, MA) and the blot was hybridized using a random-primer-labeled cDNA insert or an oligonucleotide probe. Hybridization was performed as reported by Van Damme et al. (1996). An RNA ladder (0.16–1.77 kb) was used as a marker.

Molecular Modeling

Program CLUSTAL X (Thompson et al., 1997), SeqVu (J. Gardner, J, 1995, The Garvan Institute of Medical Research, Sydney) and MACCLADE (Maddison and Maddison, 1992) were used to compare the amino acid sequences of the A and B chains of IRA with those of other RIP and to build a parsimony phylogenetic tree. A bootstrap analysis was also performed to assess the statistical significance of the parsimony tree.

HCA (Gaboriaud et al., 1987; Lemesle-Varloot et al., 1990) was performed to delineate the structurally conserved α-helices and β-sheets along the amino acid sequences of the A and B chains of IRA using ricin as a model. HCA plots were generated with the program HCA Plot2 (Doriane, Paris).

Molecular modeling of the A and B chains of IRA was carried out on a Silicon Graphics O2 R10000 workstation, using the programs INSIGHTII, HOMOLOGY, and DISCOVER3 (MSI, San Diego) as described for other type 2 RIPs (Van Damme et al., 1996, 1997b, 2000). The atomic coordinates of ricin (code 2AAI of the RCSB Protein Data Bank; Rutenber et al., 1991) were used to build the three-dimensional models of both chains. PROCHECK (Laskowski et al., 1993) was used to check the stereo-chemical assessment of the three-dimensional model. The program TURBOFRODO (Bio-Graphics, Marseille, France) was run on the Silicon Graphics O2 workstation to draw the Ramachandran plot of the modeled IRA and to perform the superposition of the models. Cartoons were rendered using Molscript (Kraulis, 1991).

Docking of Gal (Gal), *N*-acetylgalactosamine (GalNAc), and Man in the binding sites of the IRA B chain was performed with the docking menu of the HOMOLOGY program. The lowest apparent binding energy (E_{bind} expressed in kcal mol^{-1}) compatible with the hydrogen bonds (considering Van der Waals interactions and strong [2.5 Å $<$ dist(D-A) $<$3.1 Å and 120° $<$ ang(D-H-A)] and weak [2.5 Å $<$ dist(D-A) $<$3.5 Å and 105° $<$ ang(D-H-A) $<$120°] hydrogen bonds; with D, donor; A, acceptor; and H, hydrogen) found in the ricin-lactose complex (Rutenber and Robertus, 1991) was calculated with the cvff forcefield and used to anchor the pyranose ring of sugars into the binding sites of IRA. Manual docking was performed to improve the total energy associated to coulombic and Van der Waals interactions by maximizing hydrogen bonding and avoiding any steric hindrance.

ACKNOWLEDGMENTS

We would like to thank Prof. J. Balzarini and L. Van Berckelaer (Rega Institute, Katholieke Universiteit Leuven) for performing the cytotoxicity tests.

Received September 5, 2000; returned for revision October 5, 2000; accepted October 25, 2000.

LITERATURE CITED

Barbieri L, Battelli MG, Stirpe F (1993) Ribosome-inactivating proteins from plants. Biochim Biophys Acta **1154:** 237–282

de Benito FM, Citores L, Iglesias R, Ferreras JM, Soriano F, Arias J, Mendez E, Girbes T (1995) Ebulitins: a new family of type 1 ribosome-inactivating proteins (rRNA *N*-glycosidases) from leaves of *Sambucus ebulus* L. that coexist with the type 2 ribosome-inactivating protein ebulin 1. FEBS Lett **360:** 299–302

de Benito FM, Iglesias R, Ferreras JM, Citores L, Camafeita E, Mendez E, Girbes T (1998) Constitutive and inducible type 1 ribosome-inactivating proteins (RIPs) in elderberry (*Sambucus nigra* L.). FEBS Lett **428:** 75–79

Dubois M, Gilles KA, Hamilton JK, Rebers PA, Smith F (1956) Colorimetric method for determination of sugar and related substances. Anal Chem **28:** 350–356

Endo Y, Tsurugi K (1987) RNA *N*-glycosidase activity of ricin A chain: mechanism of action of the toxic lectin ricin on eukaryotic ribosomes. J Biol Chem **262:** 8128–8130

Gaboriaud C, Bissery V, Benchetrit T, Mornon JP (1987) Hydrophobic cluster analysis: an efficient new way to compare and analyze amino acid sequences. FEBS Lett **224:** 149–155

Girbes T, Citores L, Ferreras JM, Rojo MA, Iglesias R, Munoz R, Arias FJ, Calonge M, Garcia JR, Mendez E (1993) Isolation and partial characterization of nigrin b, a non-toxic novel type 2 ribosome-inactivating protein from the bark of *Sambucus nigra* L. Plant Mol Biol **22:** 1181–1186

Kraulis PJ (1991) Molscript: a program to produce both detailed and schematic plots of protein structures. J Appl Cryst **24:** 946–950

Laskowski RA, MacArthur MW, Moss DS, Thornton JM (1993) PROCHECK: a program to check the stereochemistry of protein structures. J Appl Cryst **26:** 283–291

Lehar SM, Pedersen JT, Kamath RS, Swimmer C, Goldmacher VS, Lambert JM, Blättler WA, Guild BC (1994) Mutational and structural analysis of the lectin activity in binding domain 2 of ricin B chain. Protein Engin **7:** 1261–1266

Lemesle-Varloot L, Henrissat B, Gaboriaud C, Bissery V, Morgat A, Mornon JP (1990) Hydrophobic cluster analysis: procedure to derive structural and functional information from 2-D representation of protein sequences. Biochimie **72:** 555–574

Ling J, Liu W-Y, Wang TP (1995) Simultaneous existence of two types of ribosome-inactivating proteins in the seeds of *Cinnamonum camphora*: characterization of the enzymatic activities of these cytotoxic proteins. Biochim Biophys Acta **1252:** 15–22

Maddison WP, Maddison DR (1992) MacClade: Analysis of Phylogeny and Character Evolution, Version 3.0. Sinauer Associates, Sunderland, MA

Mehta AD, Boston RS (1998) Ribosome-inactivating proteins. *In* J Bailey-Serres, DR Gallie, eds A Look Beyond Transcription: Mechanisms Determining mRNA Stability and Translation in Plants. American Society of Plant Physiologists, Rockville, MD, pp 145–152

Mierendorf RC, Pfeffer D (1987) Direct sequencing of denatured plasmid DNA. Methods Enzymol **152:** 556–562

Mo H, Van Damme EJM, Peumans WJ, Goldstein IJ (1994) Isolation and characterization of an *N*-acetyl-D-galactosamine-binding lectin from Dutch Iris bulbs which recognizes the blood group A disaccharide (GalNAcα1–3Gal). J Biol Chem **269:** 7666–7673

Peumans WJ, Van Damme EJM (1995) Lectins as plant defense proteins. Plant Physiol **109:** 347–352

Rutenber E, Katzin BJ, Collins EJ, Mlsna D, Ready MP, Robertus JD (1991) Crystallographic refinement of ricin to 2.5 Å. Proteins **10:** 240–250

Rutenber E, Robertus JD (1991) Structure of Ricin B-chain at 2.5 Å resolution. Proteins **10:** 260–269

Sambrook J, Fritsch EF, Maniatis T (1989) Molecular Cloning: A Laboratory Manual. Cold Spring Harbor Laboratory Press, Cold Spring Harbor, NY

Sanger F, Nicklen S, Coulson AR (1977) DNA sequencing with chain terminating inhibitors. Proc Natl Acad Sci USA **74:** 5463–5467

Thompson JD, Gibson TJ, Plewniak F, Jeanmougin F, Higgins DG (1997) The CLUSTAL-X windows interface: flexible strategies for multiple sequence alignment aided by quality analysis tool. Nucleic Acids Res **15:** 4876–4882

Van Damme EJM, Barre A, Barbieri L, Valbonesi P, Rouge P, Van Leuven F, Stirpe F, Peumans WJ (1997a) Type 1 ribosome-inactivating proteins are the most abundant proteins in iris (*Iris hollandica* var. Professor Blaauw) bulbs: characterization and molecular cloning. Biochem J **324:** 963–970

Van Damme EJM, Barre A, Rougé P, Van Leuven F, Peumans WJ (1996) The NeuAc (α-2, 6)-Gal/GalNAc binding lectin from elderberry (*Sambucus nigra*) bark, a type 2 ribosome inactivating protein with an unusual specificity and structure. Eur J Biochem **235:** 128–137

Van Damme EJM, Hao Q, Charels D, Barre A, Rougé P, Van Leuven F, Peumans WJ (2000) Characterization and molecular cloning of two different type 2 ribosome-inactivating proteins from the monocotyledonous plant *Polygonatum multiflorum*. Eur J Biochem **267:** 2746–2759

Van Damme EJM, Peumans WJ, Barre A, Rougé P (1998) Plant lectins: a composite of several distinct families of structurally and evolutionary related proteins with diverse biological roles. Crit Rev Plant Sci **17:** 575–692

Van Damme EJM, Roy S, Barre A, Rougé P, Van Leuven F, Peumans WJ (1997b) The major elderberry (*Sambucus nigra*) fruit protein is a lectin derived from a truncated type 2 ribosome-inactivating protein. Plant J **12:** 1251–1260

Walthall BJ, Spremulli LL, Lax SR, Ravel JM (1979) Isolation and purification of protein synthesis initiation factors from wheat germ. Methods Enzymol **60:** 193–204